

EPILEPTIC BRAIN DYNAMICS AND INFORMATION FLOW

Shivkumar Sabesan¹, Levi Good^{2,3}, Leon Iasemidis², Kostas Tsakalis¹ and David Treiman³

¹Arizona State University/Department of Electrical Engineering, Tempe AZ, USA

²The Harrington Department of Bioengineering, Tempe AZ, USA, ³Epilepsy Research Laboratory, Barrow Neurological Institute, AZ, USA

shivkumar@asu.edu

Abstract: In this paper we apply the information theoretical measure of directional information flow, namely Transfer Entropy (*TE*), to quantify the spatiotemporal dynamics of information flow between a hippocampal epileptogenic focus and its surrounding areas in the limbic system. This method is applied to electroencephalographic (EEG) recordings with sub-dural and in-depth electrodes from sub-temporal cortex and hippocampus respectively in the temporal lobe in one patient with focus in the posterior hippocampus. The results from this information flow analysis reveal that the ipsilateral anterior hippocampus (anatomically close to amygdala) and the cortex are driven by the focus most consistently across seizures when secondary seizure generalization occurs. If the epileptogenic focus is driven by the anterior hippocampus, reduced generalization of seizures is observed. These results indicate the potential of the *TE* for the identification of specific brain structures that play a critical role in the initiation, spread and control of epileptic seizures.

1. Introduction

Epilepsy is a devastating disease affecting approximately 1% of the world's population. Though anticonvulsant drug therapy is an effective tool in suppressing seizures, at least 25% of the patients are either unresponsive to medication or suffer major side effects [1]. Resective surgery is often recommended for medically intractable (pharmaco-resistant) epilepsy. However, not all patients are amenable to surgery.

Recently, electrical stimulation of the epileptogenic focus has been considered as an effective therapeutic alternative to resection [2]. However, the mechanism of its action is an open question for the researchers. While some previous studies have shown that vagus nerve stimulation significantly improves seizure control in approximately one-third of the patients with complex partial seizures [3],[4], some other studies have shown that certain forms of electrical stimulation actually induce epileptogenesis [5]. For example, repetitive stimulation in the amygdala results in kindling [5], and hippocampal stimulation with high intensity, either with high or low frequencies, induces self-sustained synchronic discharges (afterdischarges) that may be accompanied by clinical seizures [6].

From these and other studies, it is clear that the type and extent of electrical neuromodulation of the functional

connections in the brain can either initiate or suppress epileptic activity. Therefore, it can be postulated that the knowledge of the functional connectivity between different brain structures could provide useful insights into the mechanism of epileptogenesis and improve the design and implementation of effective seizure control strategies. Moreover, a better understanding of the brain's networks, that are involved in the endogenous control of epileptogenicity, could lead to identification of key targets which, when stimulated, could effectively modulate the information flow (functional neural connectivity) between the involved pathological areas to abort seizures.

In this paper, we take a driver-driven system approach to quantify the interactions between the epileptogenic focus and its surrounding brain areas. This is achieved by applying the method of Transfer Entropy (*TE*) (see [7],[8]) to electroencephalographic (EEG) recordings with sub-dural and in-depth electrodes from the right posterior hippocampus (PH), the right anterior hippocampus (AH) and the right sub-temporal cortex (STC) in one patient with temporal lobe epilepsy. In the unifocal patient we analyzed, the epileptogenic focus resided in the right PH, and therefore, its functional interactions with the ipsilateral AH and STC were then studied. In Section 2, we briefly describe the recording procedures and the application of the method of Transfer Entropy to EEG data. Results from the application of our method are presented in section 3. Discussion of these results and conclusions are given in sections 4 and 5 respectively.

2. Materials and Methods

A. Recording Procedure and EEG Data

The patient chosen for our analysis had 24 seizures with seizure onset in the right PH (seizure focus in all seizures). This patient underwent stereotactic placement of bilateral depth electrodes RTD 1, 2, 3, 4, 5 and LTD1, 2, 3, 4, 5 ((RTD1 adjacent to the right AH and LTD1 adjacent to the left AH; the remainder of the electrodes extending posteriorly in the PH). Sub-temporal strips were placed adjacent to STC with LST1 and RST1 being most mesial and LST4 and RST4 most lateral (see Fig. 1 for our typical electrode montage). Due to a predominant right PH focus in this patient, recordings only from electrodes close to the right AH, right PH (RTD2 through RTD5) and right STC (RST1 through RST4) were

analyzed.

B. Transfer Entropy (TE)

Transfer Entropy (TE) is an information theoretic approach to identify the direction of information flow and quantify the strength of coupling between linear or nonlinear systems. TE from the driving process Y to the driven process X, as first introduced in [9], is given by:

$$TE(Y \rightarrow X) = \sum_{n=1}^N P(x_{n+1}, x_n^{(k)}, y_n^{(l)}) \log \frac{P(x_{n+1} | x_n^{(k)}, y_n^{(l)})}{P(x_{n+1} | x_n^{(k)})} \quad (1)$$

where $P(x_{n+1} | x_n^{(k)})$ is the a priori transition probability of process X and $P(x_{n+1} | x_n^{(k)}, y_n^{(l)})$ is the true underlying transition probability of the combined process of X and Y. The values of the parameters k and l are the orders of the Markov process for the two coupled processes X and Y respectively. The value of N denotes the total number of points in the state space.

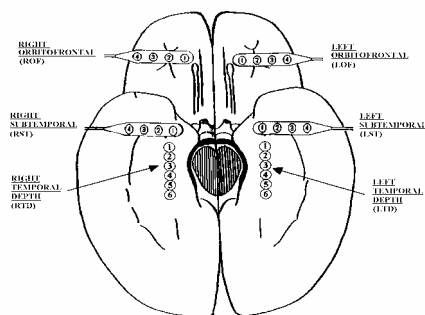


Fig.1. Schematic diagram of the depth and subdural electrode placement. This view from the inferior aspect of the brain shows the approximate location of depth electrodes, oriented along the anterior-posterior plane in the hippocampi (RTD - right temporal depth, LTD - left temporal depth), and subdural electrodes located beneath the orbitofrontal and subtemporal cortical surfaces (ROF - right orbitofrontal, LOF - left orbitofrontal, RST- right subtemporal, LST- left subtemporal).

We have recently shown that the selection of k , l and neighbourhood size (radius r) in the state space (r is used for the calculation of the involved joint and conditional probabilities via the correlation integral $C(r)$), play a critical role in obtaining reliable values for the TE from complex signals generated by systems of coupled, nonlinear (chaotic) oscillators [7]. An improved computation scheme of TE is also suggested in [7]. This method was later modified to study epileptogenic focus localization from EEG data [8].

C. Temporal information flow analysis

For the estimation of TE from EEG data, following [8], the value of k (Markov order of the driven system) was estimated for every EEG segment using the autocorrelation time constant metric. The value of l (Markov order of the driving system) was chosen to be 1. For estimation of r (neighbourhood size in the state space), a training set of five seizures was used to identify the quasi-linear region of the curve $\ln C(r)$ vs. $\ln r$ where $C(r)$ is the correlation integral in the combined state space of the driver and driven system. It was found that, on average, the quasi-linear region existed around $(-0.3 \pm -0.1 < \ln r \leq 0.2 \pm 0.1)$. A value of $\ln r^* = -0.3$ was chosen

in the estimation of the probabilities for TE in all the remaining seizures.

From data collected, only the ones around seizures that had more than one hour of inter-seizure interval were selected for analysis. A total of 15 out of 19 seizures from one of our patients with temporal lobe epilepsy matched the selection criterion (seizures at least one hour apart) and were analyzed.

TE was estimated from successive, non-overlapping EEG segments of 10.24 seconds in duration for a total of 90 minutes around every seizure (60 minutes pre-ictal, 30 minutes postictal). One value of TE for every electrode pair in both directions ($X \rightarrow Y$ and $Y \rightarrow X$) per 10.24 seconds EEG segment was then calculated for all possible pairs over time.

Statistical Significance of TE

The statistical significance of the values of TE was tested using the method of surrogate analysis. Since TE calculates the direction of information transfer between systems by quantifying their conditional statistical dependence, a random shuffling, applied only to the original driver data series (e.g. Y), destroys the temporal correlation and significantly reduces the information flow $TE(Y \rightarrow X)$. The shuffling was based on generation of white Gaussian noise and reordering of the original data samples according to the order indicated by the generated noise values. The null hypothesis that the obtained values of TE over time are not statistically significant was then tested. Transfer entropy TE_s values of the shuffled datasets, from all pairs of electrodes were obtained. A total of 12 surrogate data series over time were produced in both directional interactions for every electrode pair. The TE_s values were calculated at the optimal radius r^* estimated from the original data. For every segment of EEG data, if the TE_o values (obtained from the original time series) were greater than 3.11 standard deviations from the mean of the TE_s values, the null hypothesis was rejected at $\alpha=0.01$ (11 degrees of freedom). Only the statistically significant values of TE over time and space of electrode pairs were considered for further information flow analysis. As an illustration of results of this procedure, Table 1 shows the means and standard deviations of TE_s , TE_o and p value of four directional electrode pair interactions between AH and STC for one 10.24 sec segment of EEG data.

TABLE 1. Surrogate analyses of Transfer Entropy (* denotes the significant interactions at $p < 0.01$)

Direction of flow	Transfer Entropy (TE)		TE _o -TE _s (in standard deviation units)	p value of t-test
	Surrogate Data (TE _s) (bits)	Original Data (TE _o) (bits)		
AH→STC1*	0.01 ± 0.001	0.11	87.2	.0001
AH→STC2*	0.02 ± 0.001	0.26	165.7	.0001
STC1→AH	0.30 ± .80	.50	.25	.1137
STC2→AH	0.41 ± 0.76	0.01	0.49	.1188

From Table 1, the null hypothesis is rejected for the AH→STC1, AH→STC2 interactions. Therefore, only these interactions at that window in time were considered for further analysis (see below). We then extended our analytical procedure to include pair-wise spatial interactions between groups of electrodes from different brain areas.

D. Spatial information flow analysis

For a brain area i , and a window $W_t \in [t, t+10]$ seconds (2048 EEG data points), we define the Spatially Averaged Transfer Entropy ($SATE$) from area i to area j as

$$SATE^t(i \rightarrow j) = \frac{1}{N_i N_j} \sum_{a1=1}^{N_i} \sum_{a2=1}^{N_j} TE^t(a1 \rightarrow a2) \quad (2)$$

where N_i and N_j are the number of electrodes in areas i and j respectively. One value of $SATE$ is estimated for every area pair by averaging all its electrode pair TE values per 10.24 seconds of EEG segment. The $SATE(i, j)$ is then calculated over successive 10.24 sec EEG segments. The temporal values of $SATE$ are subsequently averaged to obtain one value for the pre-ictal period ($\hat{SATE}^{pre}(i \rightarrow j)$) and one value for the postictal period ($\hat{SATE}^{post}(i \rightarrow j)$) per area pair $i \rightarrow j$. To further enhance our understanding of the network of information flow, the value of the Spatially Averaged Net Flow ($SANF$) from area i to area j , $SANF^t(i \rightarrow j) = SATE^t(ij) - SATE^t(ji)$ was estimated and the index

$$SANF^t(i \rightarrow j) = \frac{\hat{SANF}^t(i \rightarrow j)}{\hat{\sigma}_d / \sqrt{N}} \quad (3)$$

of spatially and temporally averaged netflow from area i to area j was defined. $SANF^t(i \rightarrow j)$ is asymptotically distributed as a t-distribution with $N-1$ degrees of freedom. Since the duration of the preictal period considered herein was 1 hour versus 0.5 hour for the postictal period, $SANF^{pre}$ values greater than 4.44 and less than -4.44 were considered significant at $\alpha=0.001$ (359 degrees of freedom), and $SANF^{post}$ values greater than 4.04 and less than -4.04 were considered significant at $\alpha=0.001$ (179 degrees of freedom). We next present the results from the application of this information flow analysis to EEG.

3. Results

A. Spatio-Temporal Dynamics of TE

TE values, estimated from interictal (away from seizures) and peri-ictal (preictal, ictal and postictal) recordings were monitored to observe changes over time in the direction and strength of information flow between sites from the three areas PH, AH and STC. Fig.2 shows the smoothed TE values over time in one interictal period for all possible pairs of electrodes located in the PH, AH and

STC areas. It is clear from Fig.2 that low TE values exist in every electrode pair during the interictal period, indicating a weak bi-directional information exchange, even with the focal area (PH). This implies a “dormant” epileptogenic focus interictally. For a peri-ictal recording, it can be seen in Fig.3 that, compared to the interictal TE values, there is an increase in the TE values of all pairs of analyzed electrodes. Especially, we observe an increase in the TE (PH→STC) and TE (PH→AH) prior to a seizure, indicating a strong uni-directional flow from the focus to the ipsilateral AH and STC. An accompanying preictal increase in both TE (AH→STC) and TE (STC→AH) indicates a bi-directional flow between AH and STC prior to a seizure. During the seizure, an increase in the TE for the majority of electrode pairs is observed. Postictally, low TE in the majority of electrode pairs is observed indicating a reduced information flow, approximating interictal TE values. Next, we describe the results obtained from information flow analysis at the higher spatial level (areas).

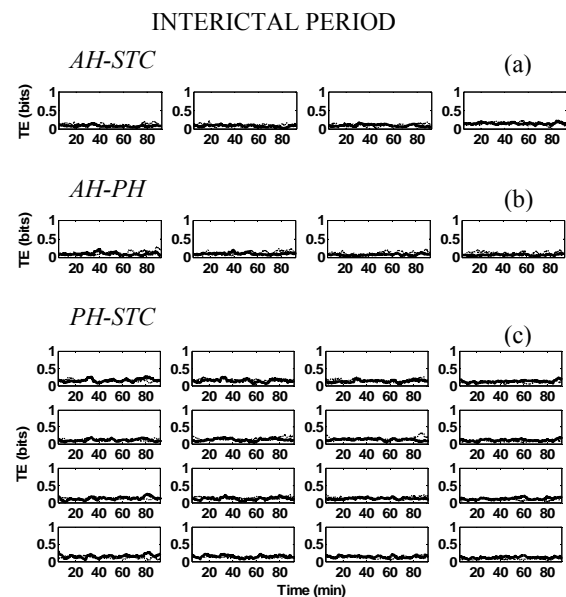


Fig.2. Smoothed TE (bits) over time estimated every 10.24 sec (non-overlapping windows) from interictal data (a) between AH and STC (AH →STC (solid line) and STC→AH (dotted line)) (b) between AH and PH (AH →PH (solid line) and PH→AH (dotted line)) (c) between PH and STC (PH →STC (solid line) and STC→PH (dotted line)). Low TE values over time between electrodes placed in PH, STC and AH indicates a weak bi-directional information exchange between the different brain areas in the interictal period.

B. Analysis of PH-AH-STC Information Flow Network

Fig.4 shows the $SATE$ values over time in the perictal period of seizure #9 for the AH-PH, AH-STC and the PH-STC pairs of areas. It is clear that there is an increase of $SATE$ (PH→AH) and $SATE$ (PH→STC), indicating a strong uni-directional flow of information from the epileptogenic focus (PH) to AH and STC preictally. A bi-directional flow exists between AH and STC prior to the seizure. In general, there is an increase in the information flow between all areas during the ictal state. Postictal

trends in information flow like the ones detected in *TE* of pairs of electrode sites are not clearly discernible from *SATE* values. The *SATE* and *SANF* values for the preictal and postictal periods of all seizures analyzed in this patient are tabulated in Table 2.

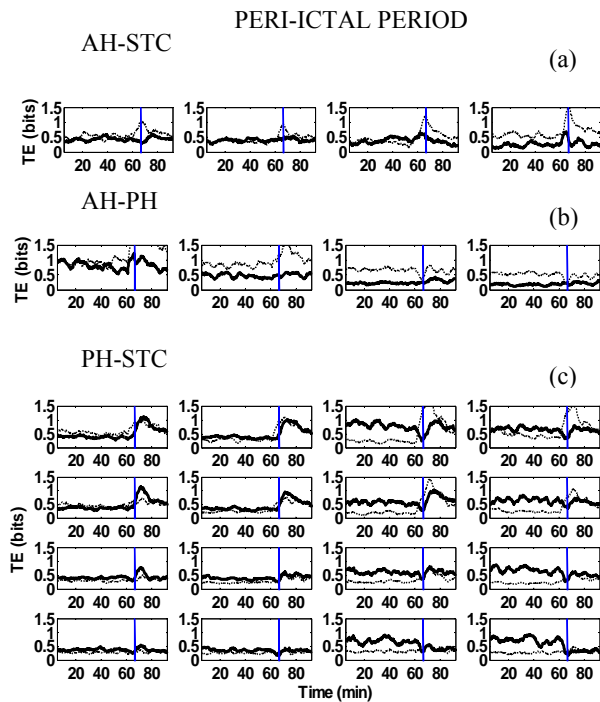


Fig.3. Smoothed *TE* (bits) over time estimated every 10.24 sec of peri-ictal data around seizure #9 (a) AH→STC (solid line) and STC→AH (dotted line) (b) AH→PH (solid line) and PH→AH (dotted line) (c) PH→STC (solid line) and STC→PH (dotted line). Blue vertical lines represent the onset of the seizure. The seizure typically lasts between 2 to 3 minutes. We observe an increase in the *TE* (PH→STC) and *TE* (PH→AH) prior to the seizure indicating a strong uni-directional flow from the focus to the anterior hippocampus and sub-temporal cortex preictally. An increase in both *TE* (AH→STC) and *TE* (STC→AH) preictally signifies a bi-directional flow between AH and STC prior to the seizure. There is an increase in *TE* values for a majority of electrode pairs during the seizure. A trend towards low postictal *TE* values in a majority of electrode pairs is also observed, indicating a weak bidirectional flow that approximates the level of interictal *TE* values.

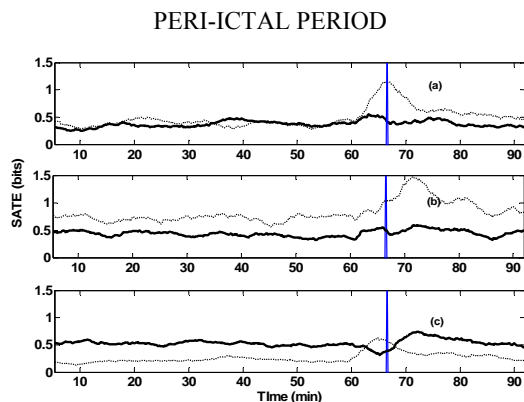


Fig.4. Smoothed *SATE* (bits) over time estimated every 10.24 sec in the perictal period of seizure #9, between (a) AH and STC (AH→STC (solid line), STC→AH (dotted line)) (b) AH and PH (AH→PH (solid

line), PH→AH (dotted line)) (c) PH and STC (PH→STC (solid line), STC→PH (dotted line)). We clearly observe an increase of *SATE* (PH→AH) and *SATE* (PH→STC) prior to this seizure, indicating a strong uni-directional flow of information from the epileptogenic focus (PH) to AH and STC preictally, while a statistically significant bi-directional flow exists between AH and STC. There is an increase in the information flow between all areas during the ictal state. Postictal trends in information flow were not clearly discernible from *SATE* values.

In Table 2, all significant *SANF^{pre}* values between different area pairs are given with a color coding scheme. The significant *SANF* (PH-AH) area pairs are marked with a red color, *SANF* (PH-STC) with blue, and *SANF* (AH-STC) with a bolded black color. Based on the *SANF^{pre}* values, we postulate three major information flow configurations that preictally may exist in the PH-AH-STC network. Flow configuration 1 shows a clear evidence of strong uni-directional flows from PH to AH and PH to STC, while the other interactions vary in their strength and direction of flow. Such a network was observed in 8 out of 15 seizures (see Table 2). Flow configuration 2 is an extension of configuration 1 with an additional strong uni-directional connection, from AH to STC. This configuration was observed in 6 out of 15 seizures (see Table 2). In flow configuration 3, we observe strong uni-directional flows, from AH to PH, AH to STC and PH to STC, while the other interactions vary in their strength and direction. Such a flow configuration existed in 4 out of 15 seizures. Fig.6 illustrates the three flow configurations observed preictally in the analyzed seizures and one exemplary flow configuration in the interictal period. The solid arrows indicate strong information flows and dashed arrows denote weak ones.

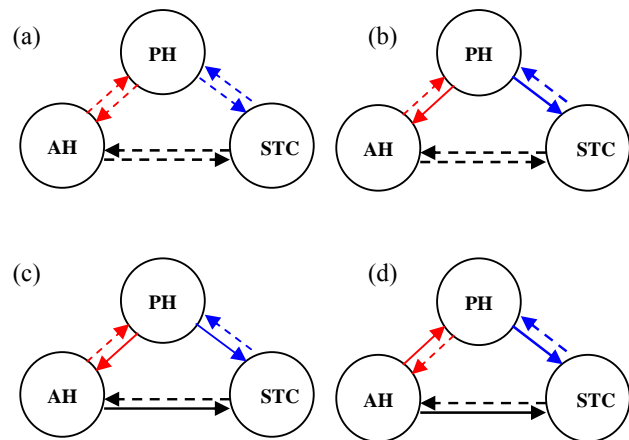


Fig.6. Flow configurations between areas PH, AH and STC.(a) *SANF* flow configuration from interictal state (b) *SANF* type 1 flow configuration from peictal state of seizure #7. (c) *SANF* type 2 flow configuration from peictal state of seizure #11. (d) *SANF* type 3 flow configuration from peictal state of seizure #14. (Solid arrows indicate stronger interactions). It is interesting to note that we observe more of type 3 interactions as seizures progress to the end of the record

TABLE 2. Spatial information flow analysis of 15 seizures in one patient (Red blue and bolded black colors denote the significant PH-AH, PH-STC and AH-STC interactions respectively at $p < 0.001$)

PATIENT 1 SEIZURE NO.	Spatially Averaged Transfer Entropy (SATE)							Spatially Averaged Net Flow (SANF)						
	$\hat{SATE}^{pre}(i \rightarrow j)$ (bits)			$\hat{SATE}^{post}(i \rightarrow j)$ (bits)				$SANF^{pre}(i \rightarrow j)$			$SANF^{post}(i \rightarrow j)$			
		Driven												
	Driving	AH	STC	PH	AH	STC	PH	AH	STC	PH	AH	STC	PH	
1	Driving	AH	0.00	0.55	0.47	0.00	0.58	0.62	0.00	-9.65		0.00	0.37	
		STC	0.77	0.00	0.30	0.57	0.00	0.39		0.00	1.86		0.00	
		PH	0.88	0.27	0.00	0.81	0.46	0.00	13.18		0.00	5.44	0.00	
2	Driving	AH	0.00	0.57	0.32	0.00	0.65	0.55	0.00	1.84		0.00	4.84	
		STC	0.54	0.00	0.25	0.55	0.00	0.42		0.00	0.31		0.00	
		PH	0.46	0.26	0.00	1.04	0.52	0.00	5.87		0.00	12.91	0.00	
3	Driving	AH	0.00	0.40	0.26	0.00	0.39	0.36	0.00	4.46		0.00	-2.05	
		STC	0.34	0.00	0.19	0.42	0.00	0.30		0.00	-6.80		0.00	
		PH	0.42	0.24	0.00	0.70	0.34	0.00	6.61		0.00	9.76	0.00	
4	Driving	AH	0.00	0.33	0.28	0.00	0.37	0.27	0.00	-5.39		0.00	-10.59	
		STC	0.41	0.00	0.22	0.58	0.00	0.28		0.00	-1.02		0.00	
		PH	0.45	0.23	0.00	0.59	0.25	0.00	6.22		0.00	10.93	0.00	
5	Driving	AH	0.00	0.43	0.36	0.00	0.31	0.27	0.00	5.26		0.00	-3.66	
		STC	0.37	0.00	0.20	0.37	0.00	0.23		0.00	-8.60		0.00	
		PH	0.49	0.28	0.00	0.50	0.24	0.00	5.78		0.00	9.01	0.00	
6	Driving	AH	0.00	0.49	0.34	0.00	0.32	0.25	0.00	9.63		0.00	-7.51	
		STC	0.37	0.00	0.17	0.45	0.00	0.22		0.00	-13.66		0.00	
		PH	0.38	0.28	0.00	0.40	0.25	0.00	2.03		0.00	7.77	0.00	
7	Driving	AH	0.00	0.36	0.30	0.00	0.38	0.25	0.00	-2.23		0.00	-14.48	
		STC	0.39	0.00	0.15	0.66	0.00	0.22		0.00	-17.65		0.00	
		PH	0.50	0.31	0.00	0.44	0.28	0.00	9.72		0.00	9.07	0.00	
8	Driving	AH	0.00	0.35	0.30	0.00	0.49	0.31	0.00	0.13		0.00	-20.88	
		STC	0.35	0.00	0.13	0.93	0.00	0.30		0.00	-20.81		0.00	
		PH	0.47	0.33	0.00	0.56	0.34	0.00	8.66		0.00	10.16	0.00	
9	Driving	AH	0.00	0.52	0.40	0.00	0.49	0.28	0.00	-1.97		0.00	-22.38	
		STC	0.54	0.00	0.25	1.06	0.00	0.33		0.00	-5.74		0.00	
		PH	0.56	0.31	0.00	0.50	0.37	0.00	7.53		0.00	9.90	0.00	
10	Driving	AH	0.00	0.43	0.23	0.00	0.65	0.28	0.00	4.79		0.00	-25.76	
		STC	0.37	0.00	0.12	1.28	0.00	0.41		0.00	-26.35		0.00	
		PH	0.47	0.39	0.00	0.56	0.55	0.00	13.55		0.00	13.16	0.00	
11	Driving	AH	0.00	0.65	0.23	0.00	0.64	0.32	0.00	21.49		0.00	-16.91	
		STC	0.38	0.00	0.16	1.11	0.00	0.33		0.00	-35.52		0.00	
		PH	0.66	0.51	0.00	0.58	0.50	0.00	23.72		0.00	13.09	0.00	
12	Driving	AH	0.00	0.25	0.16	0.00	0.27	0.15	0.00	21.49		0.00	20.17	
		STC	0.10	0.00	0.05	0.13	0.00	0.04		0.00	-27.24		0.00	
		PH	0.14	0.20	0.00	0.11	0.20	0.00	-1.97		0.00	-4.82	0.00	
13	Driving	AH	0.00	0.27	0.16	0.00	0.23	0.15	0.00	21.82		0.00	5.32	
		STC	0.11	0.00	0.04	0.18	0.00	0.06		0.00	-35.85		0.00	
		PH	0.10	0.23	0.00	0.11	0.20	0.00	-7.20		0.00	-5.07	0.00	
14	Driving	AH	0.00	0.29	0.20	0.00	0.44	0.28	0.00	18.43		0.00	22.46	
		STC	0.14	0.00	0.07	0.24	0.00	0.14		0.00	-23.43		0.00	
		PH	0.13	0.20	0.00	0.25	0.26	0.00	-6.15		0.00	-2.12	0.00	

15	AH	0.00	0.28	0.24	0.00	0.32	0.19	0.00	18.80	0.00	20.10
	STC	0.14	0.00	0.10	0.15	0.00	0.07	0.00	-20.44	0.00	-22.80
	PH	0.16	0.24	0.00	0.14	0.19	0.00	-5.28	0.00	-4.95	0.00

4. Discussion

Information flow analysis of the EEG data recorded from posterior hippocampus (PH), anterior hippocampus (AH) and the sub-temporal cortex (STC) detected a weak, bidirectional flow between all area pairs during the interictal period. There was no prominent driver, which may be indicative of a passive epileptogenic focus during the interictal period. However, a strong unidirectional information flow from PH (focal) to AH and STC emerges in the preictal period for the majority of the seizures analyzed (see configuration 1). In some seizures, a unidirectional information flow is observed from AH to STC (see configuration 2). This indicates that the epileptogenic focus (here PH) initiates the seizure activity and spreads it either directly to AH and STC or indirectly to STC through AH. From visual inspection of the EEG, it was clear that seizures with type 1 and type 2 preictal flow configurations generalize ictally to other contralateral areas the most.

Interestingly, in some seizures (see configuration 3), where a strong unidirectional flow existed preictally from AH to PH too, the ictal generalization was restricted to a smaller portion of the brain. Based on this and other preliminary evidence (e.g. all type 3 seizures were the last ones, after the patient started to take anti-epileptic medication to stop the seizures), we postulate that the AH (anatomically close to amygdala) might be involved in the endogenous control of the epileptogenic focus (PH) and STC. This information may be very useful in identifying key targets for electrical stimulation-based intervention techniques to stop seizures from occurring.

Spatial information flow analysis at the level of broad areas (via *SATE* and *SANF*) provided a clearer picture of the information flow between PH, AH and STC than the one from *TE* at the level of pairs of electrodes.

A change in the information flow, from a strong unidirectional one (between the focus and its surrounding areas) preictally to a weak bidirectional one postictally, supports our previous hypothesis that seizures are preceded by a pre-ictal dynamical entrainment of the seizure focus with other critical brain sites, and then are followed by these sites' disentrainment (weak bidirectional flow of information) in the postictal period [10]-[11].

5. Conclusion

We have shown for the first time, through directional information flow analysis and corresponding surrogate analysis, the functional connectivity of the epileptogenic focus with other areas in the limbic system over time. From our preliminary results of analysis (multiple seizures from one patient with temporal lobe epilepsy), it appears that driving of the AH and STC by the focus is a

common type of network that precedes a seizure event. Evidence that AH may be involved in the endogenous control of focal epileptic activity, and therefore be a useful target for electrical stimulation to control seizures, was provided. Our analytical scheme could have several potential applications to epilepsy, from development of maximum efficacy seizure control schemes to epileptogenic focus localization and seizure prediction, as well as in other fields of neurology and engineering.

ACKNOWLEDGEMENT

This project was supported by the Epilepsy Research Foundation and the Ali Paris Fund for LKS Research and Education, and National Institutes of Health (R01EB002089).

REFERENCES

- [1] R.S.Fisher, "Pharmacological Management of Neurological and Psychiatric Disorders," in *Epilepsy*, SJ Enna and JT Coyle, Eds., McGraw-Hill, New York, 1998
- [2] D.M. Durand and M Bikson, "Suppression and Control of Epileptiform Activity by Electrical Stimulation: A Review," in *Proc. IEEE*, 2001, vol. 89, pp. 1065-1082
- [3] D. Labar, J.Murphy, E. Tecoma., "Vagus nerve stimulation for medication-resistant generalized epilepsy. E04 VNS Study Group," *Neurology*, vol. 52(7), 1999, pp. 1510-1512
- [4] B. M. Uthman, B. Wilder, E.J. Hammond, and S.A. Reid, "Efficacy and safety of vagus nerve stimulation in patients with complex partial seizures," *Epilepsia*, vol. 31, 1990, pp. 603-611
- [5] G.V. Goddard, D.C McIntyre, C.K. Leech., "A permanent change in brain function resulting from daily electrical stimulation," *Exp Neurol.*, vol. 25(3), 1969, pp. 295-330
- [6] V.M. Fernandes de Lima, J.P. Pijn, C. Nunes Filipe, F. Lopes da Silva, "The role of hippocampal commissures in the interhemispheric transfer of epileptiform afterdischarges in the rat: a study using linear and non-linear regression analysis," *Electroencephalogr Clin Neurophysiol.*, vol. 76(6), 1990, pp. 520-539
- [7] S. Sabesan, K. Narayanan, A. Prasad, and L.D. Iasemidis, "Improved Measure of Information Flow in Coupled Non-Linear Systems," in *Proc. ICMS*, 2003, pp. 270-274
- [8] S. Sabesan, K. Narayanan, A. Prasad, L.D. Iasemidis, A. Spanias and K. Tsakalis, Information flow in coupled nonlinear systems: Application to the epileptic human brain," In: *Data Mining in Biomedicine*, P. Pardalos, Ed., Springer (in press).
- [9] T. Schreiber, Measuring information transfer, *Phys. Rev. Lett.*, vol. 85, 2000, 461-464
- [10] L.D. Iasemidis, D.S. Shiau, J.C. Sackellares, P.M. Pardalos and A. Prasad, "Dynamical resetting of the human brain at epileptic seizures: Application of nonlinear dynamics and global optimization techniques", *IEEE Transactions on Biomedical Engineering*, vol. 51, 2004, pp. 493-506
- [11] L.D. Iasemidis, "Epileptic seizure prediction and control", *IEEE Transactions on Biomedical Engineering*, vol. 50 (5), 2003, pp. 549-558